Chemistry and Physics of Lipids 208 (2017) 58–64

Contents lists available at ScienceDirect

Chemistry and Physics of Lipids

journal homepage: www.elsevier.com/locate/chemphyslip

Thermotropic properties of phosphatidylcholine nanodiscs bounded by styrene-maleic acid copolymers

J.J. Dominguez Pardo[a,*], J.M. Dörr[a], M.F. Renne[a], T. Ould-Braham[a], M.C. Koorengevel[a], M.J van Steenbergen[b], J.A. Killian[a,*]

[a] Membrane Biochemistry & Biophysics, Bijvoet Center for Biomolecular Research, Department of Chemistry, Faculty of Science, Padualaan 8, 3584 CH Utrecht, The Netherlands

[b] Department of Pharmaceutics, Utrecht Institute for Pharmaceutical Sciences (UIPS), Faculty of Science, Utrecht University, PO Box 80082, 3508 TB Utrecht, The Netherlands

ARTICLE INFO

Keywords:
SMA
laurdan
nanodisc
differential scanning calorimetry
lipid packing
lipid phase transition

ABSTRACT

Styrene-maleic acid copolymers (SMA) have been gaining interest in the field of membrane research due to their ability to solubilize membranes into nanodics. The SMA molecules act as an amphipathic belt that surrounds the nanodiscs, whereby the hydrophobic styrene moieties can insert in between the lipid acyl chains. Here we used SMA variants with different styrene-to-maleic acid ratio (i.e. 2:1, 3:1 and 4:1) to investigate how lipid packing in the nanodiscs is affected by the presence of the polymers and how it depends on polymer composition. This was done by analyzing the thermotropic properties of a series of saturated phosphatidylcholines in nanodiscs using laurdan fluorescence and differential scanning calorimetry. In all cases it was found that the temperature of the main phase transition (T_m) of the lipids in the nanodiscs is downshifted and that its cooperativity is strongly reduced as compared to the situation in vesicles. These effects were least pronounced for lipids in nanodiscs bounded by SMA 2:1. Unexpected trends were observed for the calorimetric enthalpy of the transition, suggesting that the polymer itself contributes, possibly by rearranging around the nanodiscs when the lipids adopt the fluid phase. Finally, distinct differences in morphology were observed for nanodiscs at relatively high polymer concentrations, depending on the SMA variant used. Overall, the results suggest that the extent of preservation of native thermodynamic properties of the lipids as well as the stability of the nanodiscs at high polymer concentrations is better for SMA 2:1 than for the other SMA variants.

1. Introduction

Styrene-maleic acid copolymers (SMA) are rapidly gaining interest as tools in membrane protein research due to their capacity of solubilizing biological membranes into nanodiscs without the need for detergents. These so-called “native nanodiscs” thus enclose membrane proteins embedded in a lipid bilayer (for review see (Dörr et al., 2016)), while retaining native protein-lipid interactions (Dörr et al., 2014; Long et al., 2013; Prabudiansyah et al., 2015; Swainsbury et al., 2014). SMA variants are commercially available differing in average length of the polymer and in average styrene-to-maleic acid ratio. The variants most frequently used in literature are SMA 2:1 (styrene-to-maleic acid ratio of 2:1) (Dörr et al., 2014; Jamshad et al., 2015; Swainsbury et al., 2014) and SMA 3:1 (Cuevas Arenas et al., 2016; Dominguez Pardo et al., 2017; Orwick et al., 2012) of approximately ~10 kDa. Studies in model membranes showed that the SMA 2:1 variant is slightly more efficient in solubilization than SMA 3:1, while both are significantly more efficient than SMA 4:1 (Scheidelaar et al., 2016). Similar results were reported for solubilization of proteins from *E.coli* (Morrison et al., 2016).

A general advantage of using SMA-bounded nanodiscs for membrane protein research is that the bilayer environment reflects the organization of the lipids in the native membrane (Jamshad et al., 2015; Orwick et al., 2012). However, for studies on membrane protein structure and function it is also important to know to what extent the packing of the lipids in the nanodiscs is preserved and resembles that in the native membrane. Previous reports showed that SMA molecules behave as a belt encircling the nanodiscs, where the styrene units intercalate between the lipid acyl chains (Jamshad et al., 2015; Orwick et al., 2012). This intercalation will affect lipid packing and it is thus likely that the properties of the nanodiscs and packing of the lipids will be affected by the composition of the SMA molecules that form the belt. This is supported by the recent observation that SMA composition

Abbreviations: SMA copolymer, styrene- maleic acid copolymer; GP, generalized polarization; DSC, differential scanning calorimetry; MLV, multilamellar vesicle

* Corresponding authors.
E-mail address: j.j.dominguezpardo@uu.nl (J.J. Dominguez Pardo).

http://dx.doi.org/10.1016/j.chemphyslip.2017.08.010
Received 21 June 2017; Received in revised form 22 August 2017; Accepted 24 August 2017
Available online 18 September 2017

affects the functional properties of proteins in purified nanodiscs (Morrison et al., 2016).

A convenient way of monitoring the extent to which native lipid packing properties are preserved in nanodiscs is by investigating the thermotropic behavior of the enclosed lipids as compared to that of lipids in vesicles (Denisov et al., 2005; Jamshad et al., 2015; Orwick et al., 2012; Shaw et al., 2004; Tanaka et al., 2015). In order to gain insight into the effect of polymer composition on the properties of the formed nanodiscs and in particular on the extent to which native membrane properties are preserved, we here directly compared the effects of different polymer variants on the thermotropic properties of SMA-bounded nanodiscs. Such a direct comparison is essential, because it is becoming increasingly clear that the properties of nanodiscs are dependent on precise experimental conditions, and can vary for example with SMA concentration (Cuevas Arenas et al., 2016; Oluwole et al., 2017).

To allow comprehensive and systematic comparison, we studied a series of saturated phosphatidylcholine lipids in SMA-nanodiscs by laurdan fluorescence and DSC analysis. Briefly, we found that lipids in SMA 2:1-nanodiscs retain to a higher extent the thermodynamic properties of the native membrane as compared to lipids in SMA 3:1-nanodiscs under a variety of experimental conditions. Moreoever, upon varying the SMA concentration both the thermodynamic properties and the morphology of the nanodiscs were best retained in SMA 2:1-nanodiscs. These results are discussed in terms of the membrane interactions of the styrene units in SMA and how they may depend on the phase state of the lipids.

2. Materials and Methods

2.1. Materials

The following lipids where purchased from Avanti Polar Lipids (Alabaster, AL, USA): 1,2-dipentadecanoyl-*sn*-glycero-3-phosphocholine (di-15:0 PC), 1,2-dipalmitoyl-*sn*-glycero-3-phosphocholine (di-16:0 PC), 1,2-diheptadecanoyl-sn-glycero-3-phosphocholine (di-17:0 PC),1,2-distearoyl-*sn*-glycero-3-phosphocholine (di-18:0 PC) and 1,2-diarachidoyl-*sn*-glycero-3-phosphocholine (di-20:0 PC). The SMA copolymers, Xiran 20010 (molar ratio of styrene-to-maleic anhydride of 4:1), Xiran 25010 (molar ratio of styrene-to-maleic anhydride of 3:1) and Xiran 30010 (molar ratio of styrene- to- maleic anhydride of 2:1), all with a weight average molecular weight of ~10 kDa, were a kind gift from Polyscope Polymers (Geleen, The Netherlands). The polymers were converted to the acid form by hydrolysis under base-catalyzed conditions as detailed before (Scheidelaar et al., 2015). Laurdan (6-dodecanoyl-2-dimethylaminonaphtalene) and all other chemicals were purchased from Sigma Aldrich (St.Louis, MO).

2.2. Preparation of multilamellar vesicles (MLVs)

Phospholipid stock solutions were prepared in chloroform/methanol (9:1 v/v) in concentrations of either 5 mM or 20 mM (for DSC measurements), based on the analysis of total phosphate (Rouser et al., 1970). A 5-mM laurdan stock solution was prepared in ethanol/chloroform (1:1 v/v). Aliquots from the phospholipid stock solutions and from the laurdan stock solutions, if required, were taken and the solvent was removed under a stream of N_2. The resulting lipid film was dried in a desiccator under vacuum for at least 1 h. Multilamellar vesicles (MLVs) were obtained by hydrating the lipid films with buffer (50 mM Tris-HCl, 150 mM NaCl, pH 8.0) to a final concentration of 0.5 mM or 20 mM (for DSC measurements). The samples were then subjected to 10 freeze-thaw cycles, each consisting of 3 min freezing in liquid N_2 (–196 °C) and 3 min thawing in a water bath above T_m of the lipids (Marsh, 2013).

2.3. Preparation of nanodiscs

Dispersions of MLVs containing either 0.5 mM or 20 mM lipid were incubated with SMA (SMA-to-lipid mass ratios used for solubilization are detailed in the legends of each figure) for 1 h at the phase transition temperature (T_m) of the lipid components (Lewis et al., 1987; Marsh, 2013). After incubation with SMA, the samples were placed in an Optima Max ultracentrifuge (Beckman-Coulter, Brea, CA). Traces of non-solubilized material were removed by centrifugation at 115,000 × *g* for 1 h at 4 °C.

2.4. Laurdan fluorescence

Laurdan fluoresence was measured using a Varian Cary Eclipse fluorescence spectrophotometer (Santa Clara, CA). 1-mL aliquots of ~0.5 mM phosphatidylcholine nanodisc solutions (lipid-to-laurdan molar ratio of 200:1) were placed in a 10-mm quartz cuvette and excited at 340 nm. The excitation and emission slits were adjusted to 5 nm. Emission spectra were recorded in the range of 400–550 nm at a speed of 60 nm/min. The temperature was controlled with a Peltier cuvette holder (Santa Clara, CA) in the range of 5–70 °C. Exact temperatures of the samples were obtained from a thermosensor dipped inside the cuvette. Generalized polarization parameters defined as $GP = (I_{440nm}\text{-}I_{490nm})/(I_{440nm} + I_{490nm})$ (Parasassi et al., 1991) were obtained as function of temperature. Phase transition midpoints were determined by nonlinear least-squares fitting using a sigmoidal fitting function (Kemmer and Keller, 2010). GP values were obtained from a single heating scan. For selected samples additional heating cycles were performed as a control and negligible differences in the GP curves were observed.

2.5. Differential scanning calorimetry

DSC measurements were performed using a Discovery DSC (TA Instruments, Newcastle, DE) calorimeter. 10-µL aliquots of nanodisc solutions or MLV dispersions containing ~20 mM lipids were placed in hermetic Tzero pans (TA Instruments, Newcastle, DE). Heating curves were recorded in the ranges of 5–70 °C at a scan rate of 5 °C/min at least 3 times. Calorimetric enthalpies (ΔH_{cal}) were determined from the area under the peak of the main phase transition using Trios software (TA Instruments, Newcastle, DE). The calorimetric enthalpies reported represent the average obtained from the 2nd and the 3rd heat scan from 2 independent samples. Error bars reported for both T_m and ΔH_{cal} values correspond to the average from the 2nd and 3rd heating cycles from 2 independent samples.The full width at half height of the peaks ($\Delta T_{1/2}$) were determined manually using Adobe Illustrator software (San José, CA). For determination of the calorimetric enthalpy, the total lipid material contained in the calorimetric pans was recovered by perforating the pans in a glass tube containing 1-mL of water. The tubes were vortexed vigorously in order to assure that all lipids were extracted from the pans. Next, the total lipid was quantified in triplicate by applying a phosphate analysis (Rouser et al., 1970) on 200- µL aliquots of the resulting nanodisc solutions or MLV dispersions.

2.6. Transmission electron microscopy

Size characterization of di-16:0 PC and di-18:0 PC nanodiscs was performed by transmission electron microscopy (TEM). 1-mL aliquots of 0.5 mM nanodisc solutions were adsorbed on carbon-coated mica following the carbon flotation technique and stained with a staining solution containing 2% (w/v) sodium silicotungstate as detailed before (Dominguez Pardo et al., 2017). Images were taken under low dose conditions at a nominal magnification of 49,000 with a T12 electron microscope (FEI, Hillsboro, OR) at an operating voltage of 120 kV using an ORIUS SC1000 camera (Gatan, Inc., Pleasanton, CA). The average size of the nanodiscs was estimated from at least 25 well-defined

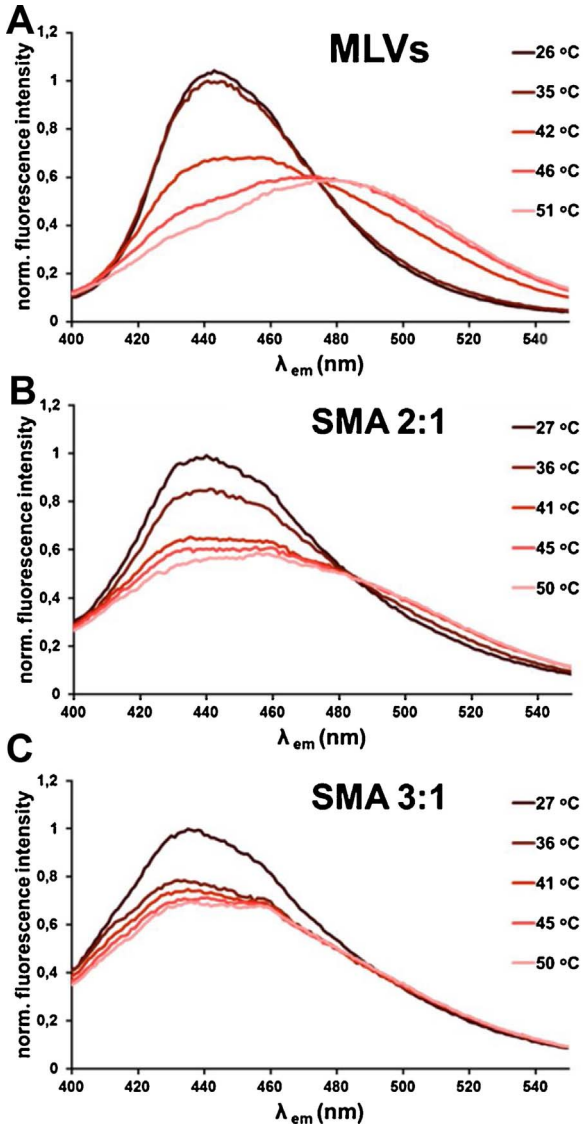

Fig. 1. Normalized fluorescence emission of laurdan molecules incorporated in di-16:0 PC self-assemblies: A) MLVs, B) SMA 2:1 nanodiscs and C) SMA 3:1 nanodiscs. Spectra were recorded using an excitation wavelength of 340 nm. The data shown correspond to the spectra obtained during the first heating cycle. Nanodiscs were obtained at a SMA-to-lipid mass ratio of ~ 1.7.

individual particles. The maximum diameter was determined using Adobe Illustrator software (San Jose, CA).

3. Results

3.1. Native thermotropic lipid properties are better retained in SMA 2:1 nanodiscs than in SMA 3:1 nanodiscs

Shifts in phospholipid phase behavior can be conveniently followed by incorporating amphipathic solvatochromic dyes, such as laurdan, into lipid membranes. Laurdan probes are extremely sensitive to solvent relaxation and can be used to track changes in membrane fluidity based on a shift in emission maximum. Briefly, when the temperature is raised above the main gel-to-fluid phase transition temperature (T_m) of the lipid constituents of the membrane, a spectral shift of the emission maximum takes place from 440 nm to 490 nm (Parasassi et al., 1991). This is illustrated in Fig. 1A where laurdan is incorporated into di-16:0 PC MLVs, which have a T_m of around 41 °C (Lewis et al., 1987). Below T_m, at 26 °C and 35 °C, the emission maximum is at 440 nm. At 42 °C,

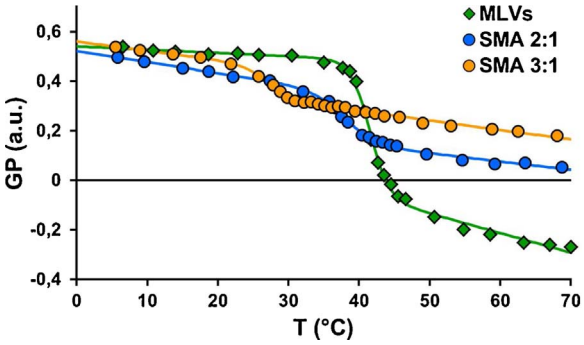

Fig. 2. Laurdan generalized polarization (GP) values of di-16:0 PC self-assembled in MLVs (green squares), SMA 2:1 nanodiscs (blue circles) and SMA 3:1 nanodiscs (orange circles). Solid lines indicate a sigmoidal fit. Nanodiscs were obtained at a SMA-to-lipid mass ratio of ~1.7.

the intensity of the emitted fluorescence is decreased at 440 nm but is increased at 490 nm. At higher temperatures of 46 °C and 51 °C, the emission maximum is completely shifted to ~490 nm.

Insight into the relative amount of gel and fluid phase present can be obtained by calculating the generalized polarization (GP) values from the maximum intensities of the two emission peaks (Parasassi et al., 1991). As shown in Fig. 2 **(green line)** for di-16:0 PC MLVs the GP values slightly decrease as the temperature is raised, with a sharp inflection around T_m, indicating that phase interconversion is taking place with a high degree of cooperativity (Parasassi et al., 1994). By applying non-linear regression analysis T_m was found to be ~41 °C.

The same experimental approach was used for nanodiscs obtained after addition of SMA to di-16:0-PC MLVs. We inititally focussed on SMA 2:1 and SMA 3:1, as they are the commonly used SMA variants in literature. As shown in Fig. 1B, for SMA 2:1 a decrease in the emission at 440 nm is observed that now begins already at lower temperatures in the range of 27 °C to 36 °C. In addition, there is no clear peak appearing at 490 nm upon further increasing the temperature. Similar but more pronounced effects are observed for di-16:0 PC SMA 3:1 nanodiscs (Fig. 1C). These results are attributed to a blue shift of the emission wavelength that is particularly pronounced in the fluid phase (Parasassi et al., 1993) and that can be ascribed to a decrease in i) the motility of laurdan molecules or ii) the polarity of the solvent (Parasassi et al., 1994; Parasassi et al., 1993). Here it is possible that both factors are involved as a result of binding of SMA molecules to the surface of the nanodiscs, which may impede the motility of the lipids (Cuevas Arenas et al., 2016) while at the same time insertion of styrene moieties will decrease the polarity.

Analysis of the GP curves observed for laurdan in the nanodiscs reveals that for SMA 2:1 nanodiscs the phase transition occurs at ~38 °C and for SMA 3:1 nanodiscs at ~27 °C (Fig. 2). The decreased steepness of the slope of the inflection curve around T_m suggests a decrease in the cooperativity of the transition. This effect is more pronounced for SMA 3:1 nanodiscs than for SMA 2:1 nanodiscs. Furthermore, the higher GP values of SMA 2:1 nanodiscs and particularly SMA 3:1 nanodiscs in the fluid phase suggest a less hydrated or more ordered environment than for MLVs.

Similar results were obtained when the lipid acyl chain length was varied from 15 to 18 C-atoms (see GP curves in Fig. S1). Overall, the Laurdan data show a downshift in T_m of ~3–5 °C for saturated phosphatidylcholines organized in SMA 2:1 nanodiscs as compared to MLVs (Table 1, left column), while the same lipids assembled in SMA 3:1 nanodiscs show a downshift of ~14–17 °C. In addition, the SMA 3:1 nanodiscs exhibit a further increased broadening of the phase transition and a less hydrated environment in the fluid phase as compared to SMA 2:1 nanodiscs for all lipids tested.

The laurdan fluorescence data were complemented with differential scanning calorimetry (DSC) analysis. DSC has the advantage of being a

Table 1
T_m values and peak widths at half maximum ($\Delta T_{½}$) of saturated phosphatidylcholine self-assemblies measured by laurdan fluorescence and DSC. DSC data are given as averages of the 2nd and 3rd heating cycle from 2 independent samples, with errors representing the standard deviation.

Phospholipid		T_m (°C) Laurdan	T_m (°C) DSC	$\Delta T_{½}$ (°C) DSC
di-15:0 PC	MLVs	34.3	33.3 ± 0.1	0.7 ± 0.1
	SMA 2:1	28.6	29.2 ± 0.2	4.0 ± 0.2
	SMA 3:1	ND*	21.6 ± 0.4	6.6 ± 0.4
di-16:0 PC	MLVs	41.4	40.8 ± 0.1	0.5 ± 0.1
	SMA 2:1	38.0	37.4 ± 0.2	3.8 ± 0.2
	SMA 3:1	27.1	29.4 ± 0.2	5.1 ± 0.1
di-17:0 PC	MLVs	48.1	48.3 ± 0.1	0.4 ± 0.1
	SMA 2:1	44.1	46.5 ± 2.0	3.3 ± 0.1
	SMA 3:1	34.1	36.1 ± 0.6	5.6 ± 0.1
di-18:0 PC	MLVs	53.3	54.0 ± 0.1	0.4 ± 0.1
	SMA 2:1	48.7	50.9 ± 0.1	2.9 ± 0.1
	SMA 3:1	36.5	42.3 ± 0.2	5.5 ± 0.1

* No clear transition is visible.

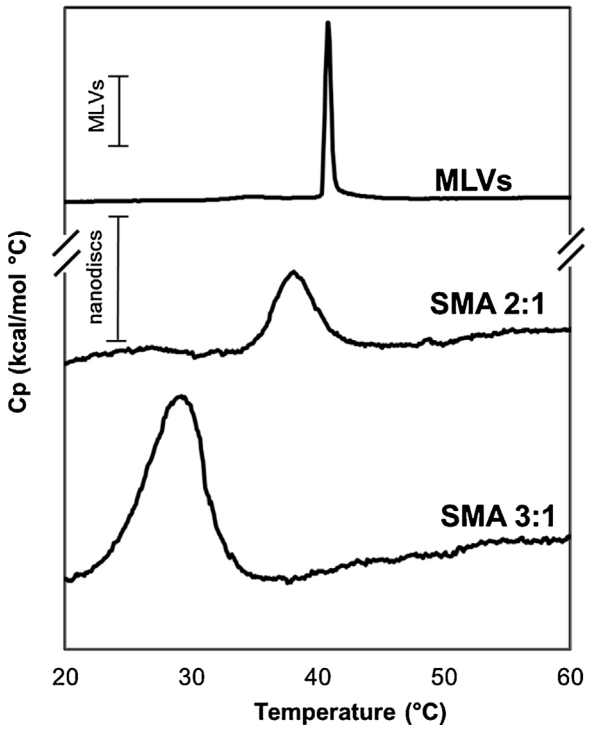

Fig. 3. Representative differential scanning calorimetry (DSC) thermograms of di-16:0 PC lipids self-assembled in MLVs, SMA 2:1 nanodiscs and SMA 3:1 nanodiscs. Nanodiscs were obtained at a SMA-to-lipid mass ratio of ~1.7. The inserted scale bar at the top (MLVs) corresponds to 5 kcal/mol °C while the bar at the bottom (nanodiscs) corresponds to 0.5 kcal/mol °C.

high precision technique which does not require the addition of fluorophores that may perturb the phase equilibrium of the membrane. As shown in Fig. 3, DSC thermograms of di-16:0 PC MLVs display a sharp peak with a maximum corresponding to T_m at ~41 °C.SMA 2:1 nanodiscs and SMA 3:1 nanodiscs both exhibit a lowering of T_m with the downshift being more pronounced in SMA 3:1 nanodiscs, as was also observed for PC lipids with shorter and longer chain lengths (Fig. S**2**). The T_m values show downshifts of approximately ~2–4 °C in T_m of lipids in SMA 2:1 nanodiscs and of ~11–13 °C in SMA 3:1 nanodiscs (Table 1, middle column). These shifts are slightly less than those observed with laurdan fluorescence, most likely due to differences in experimental conditions, but nevertheless the results are qualitatively similar.

DSC analysis also provides insight into the cooperativity of the gel-to-fluid phase transition. The narrow peak width at half maximum ($\Delta T_{1/2}$) observed for di-16:0 PC phospholipids in MLVs indicates a high degree of cooperativity (Biltonen and Lichtenberg, 1993), while the heat curves of both nanodisc samples show a clear broadening, suggesting a notable loss in the cooperativity (Denisov et al., 2005; Orwick et al., 2012; Shaw et al., 2004). The broadening is more pronounced in SMA 3:1 nanodiscs as compared to SMA 2:1 nanodiscs, as was also observed for other lipids **(Fig. S2)**. These results, as quantified in Table 1, are fully consistent with the observed effects of the polymers on the steepness of the inflection points in the laurdan GP-curves (Fig. 2 and S1).

Table 2
Calorimetric enthalpies (ΔH_{cal}) of the gel-to-fluid phase transition of saturated phosphatidylcholines. Data are given as averages obtained from the 2nd and 3rd heating cycle from 2 independent samples, with errors representing the standard deviation.

ΔH_{cal} (kcal/mol)	di-15:0 PC	di-16:0 PC	di-17:0 PC	di-18:0 PC
MLVs	7.2 ± 0.2	7.6 ± 0.1	9.4 ± 0.4	10.0 ± 0.6
SMA 2:1	1.4 ± 0.1	1.5 ± 0.2	1.8 ± 0.2	1.8 ± 0.1
SMA 3:1	3.2 ± 0.3	3.8 ± 0.1	4.8 ± 0.6	4.5 ± 0.1

3.2. Calorimetric enthalpy values of the gel-to-fluid phase transition may be determined by multiple processes

Another characteristic property of the gel-to-fluid phase transition is the molar calorimetric enthalpy (ΔH_{cal}) associated with the melting process. As displayed in Table 2, the ΔH_{cal} values for MLVs of lipids increase with lipid chain length, in line with previously reported data (Goto et al., 2009; Lewis et al., 1987; Marsh, 2013). For all lipids, a dramatic loss in calorimetric enthalpy is observed when present in SMA-bounded nanodiscs. For SMA 2:1 nanodiscs ΔH_{cal} is approximately 20% of ΔH_{cal} found in MLVs (Table 2). Rather surprisingly, the loss of ΔH_{cal} is less dramatic in SMA 3:1-nanodiscs, where ~45-50% of the value is retained.

To obtain further insight into the origin of this somewhat puzzling observation we decided to extend the systematic approach by going to system of lipids with an even longer chain length. As shown in Fig. 4, di- 20:0 PC MLVs exhibit a narrow, highly cooperative gel-to-fluid phase transition while the SMA 2:1-nanodiscs again show a broadening and a small downshift in T_m. Interestingly, a remarkable feature now occurs in the thermogram obtained for SMA 3:1-nanodiscs, where the main phase transition appears to be split into two peaks. Identical thermograms were obtained upon repeated heating showing complete reversibility of this transition. A similar, reversible effect of apparent multiple transitions was detected upon extending the data-set to include nanodiscs of SMA 4:1 copolymers, as shown for di-18:0 PC nanodiscs (Fig. S**3**). These results suggest that interpretation of effects on ΔH_{cal} in these nanodiscs is not straightforward, and that possibly SMA molecules themselves contribute to the enthalpy of the transition. We will further elaborate on these effects in the discussion.

3.3. Thermotropic properties are more sensitive to polymer concentration in nanodiscs bounded by SMA 3:1 or SMA 4:1 than in nanodiscs bounded by SMA 2:1

Next it was investigated to what extent the SMA-to-lipid ratio at which the nanodiscs are obtained may affect the thermotropic properties of the lipids in the nanodiscs. As shown in Fig. 5A, T_m of di-16:0 PC is shifted to lower temperatures as the SMA-to-lipid ratio increases. Importantly, this concentration effect seems to be less pronounced in SMA 2:1-nanodiscs than in SMA 3:1-nanodiscs and SMA 4:1-nanodiscs.

For all samples also the calorimetric enthalpy values of the gel-to-fluid transition were determined and these are shown in Fig. 5B. The results show that ΔH_{cal} corresponding to di-16:0 PC lipids bounded by

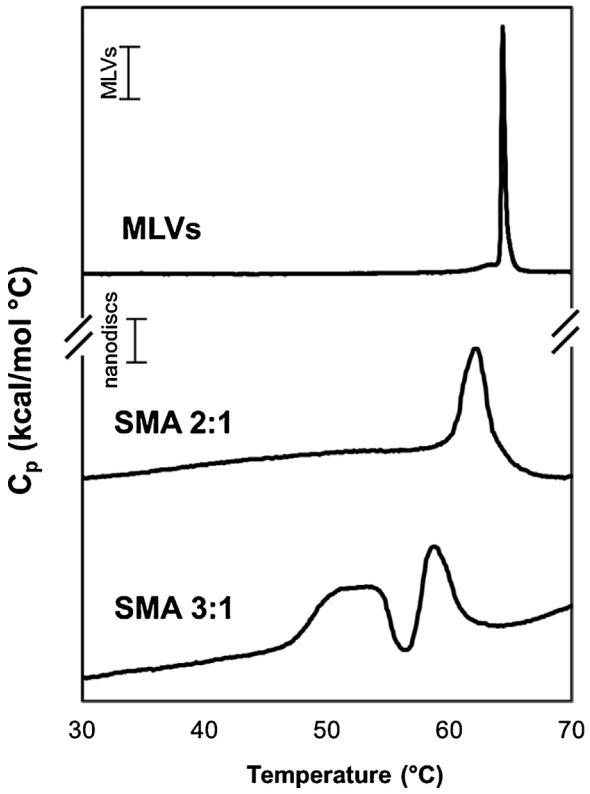

Fig. 4. Representative differential scanning calorimetry (DSC) thermograms of di-20:0 PC. Nanodiscs were obtained at a SMA-to-lipid mass ratio of ~1.7. The inserted bars at the top (MLVs) correspond to 5 kcal/mol °C and the inserted bars at the bottom (nanodiscs) correspond to 0.5 kcal/mol.

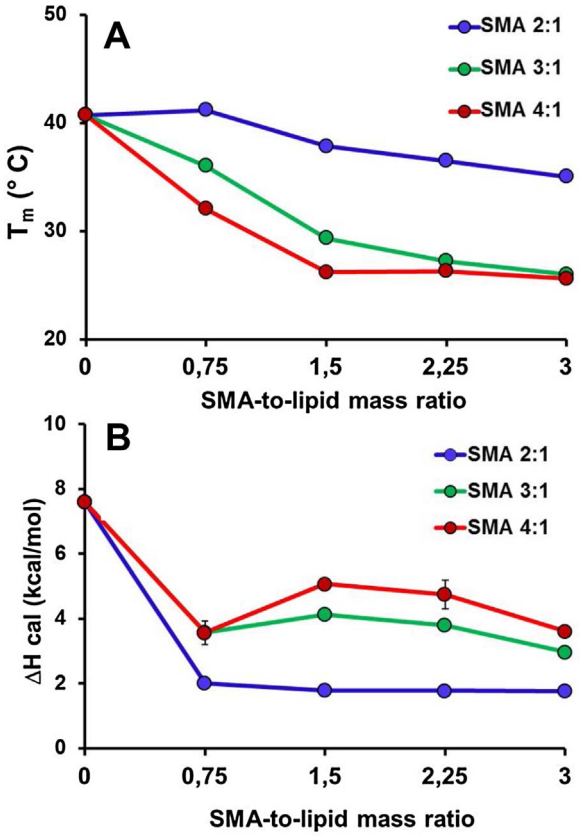

Fig. 5. Variation in A) T_m and B) ΔH_{cal} of the gel-to-fluid phase transition of di-16:0 PC lipids in nanodiscs bounded by SMA 2:1 (blue circles) SMA 3:1 (green circles) or SMA 4:1 (red circles). Data are given as averages obtained from the 2nd and 3rd heating cycle from 2 independent samples. Errors representing the standard deviation are covered by the markers.

SMA 2:1 is low and rather constant, independent of the SMA concentration used for solubilization., When either the SMA 3:1 or the SMA 4:1 variant are used, the values of ΔH_{cal} are larger and fluctuate. This fluctuation of the ΔH_{cal} values may indicate that i) other factors may be contributing energetically to the phase transition of lipids or ii) the morphology of the nanodiscs is affected by the concentration of SMA.

3.4. Morphological integrity is better preserved in nanodiscs bounded by SMA 2:1 than in nanodiscs bounded by SMA 3:1 or SMA 4:1

Finally it was investigated how the SMA variants affect the size and morphology of the nanodiscs and whether this depends on the concentration of the polymer. As illustrated in Fig. 6, nanodiscs bounded by SMA 2:1 form well-defined nanodiscs at all polymer concentrations with a somewhat inhomogeneous size distribution of approximately d ~ 9—18 nm. A remarkable feature here is the formation of phospholipid stacks. These are also known as “rouleaux” stacks and have been observed before in nanodiscs bounded by SMA molecules and MSP-like proteins (Dominguez Pardo et al., 2017; Zhang et al., 2011), where they were ascribed to an artefact resulting from the interaction between positively-charged choline head groups with the negatively-charged inorganic crystals from the staining solution. These stacks are also observed in nanodiscs bounded by SMA 3:1, where they can be seen most clearly at lower polymer concentrations (SMA-to-lipid mass ratio of 0.75 and 1.5). Here the nanodiscs are still well-defined and a size distribution is observed of 9—16 nm, similar as for SMA 2:1 nanodiscs. At higher concentrations of SMA 3:1 (SMA-to-lipid mass ratio > 1.5) the morphological integrity of the nanodiscs is affected, as shown by the formation of nanoscopic aggregates. Remarkably, EM micrographs of nanodiscs bounded by SMA 4:1 revealed a much higher degree of polydispersity as compared to the other SMA analogues and a higher tendency to aggregate. The presence of circular structures is ascribed to artifacts during the preparation of the grids. Stacks of nanodiscs are not observed in micrographs of SMA 4:1 nanodiscs. Together these data suggest that SMA 3:1 and in particular SMA 4:1 are less prone than SMA 2:1 to form well defined circular-shaped nanodiscs and that SMA 2:1-nanodiscs “allow” a high amount of SMA in solution without affecting their morphological integrity.

Similar differences in behavior between the SMA analogues were found using dynamic light scattering. These experiments (**Figure S 4**) revealed rather homogeneous hydrodynamic diameter distributions for nanodiscs bounded by either SMA 2:1 and SMA 3:1 (d ~ 9—12 nm), and a heterogeneous size distribution for SMA 4:1 nanodiscs at the various SMA concentrations.

4. Discussion

In this study we analyzed the thermotropic properties of saturated phosphatidylcholines in nanodiscs that are bounded by SMA with a styrene-to-maleic acid ratio of 2:1, 3:1 or 4:1. Laurdan fluorescence as well as DSC results for lipids with varying acyl chain length showed that the native main phase transition temperature (T_m) of the lipids is downshifted in the SMA-bounded nanodiscs as compared to the situation in large multilamellar vesicles, and that the cooperativity of the gel-to-fluid phase transition is highly reduced. Nevertheless, native-like properties seemed best preserved in SMA 2:1 nanodiscs, where in all lipid systems the effects on T_m and broadening were least profound. In theory, a likely explanation would be that SMA 2:1 nanodiscs have a somewhat larger size than SMA 3:1 or SMA 4:1 nanodiscs. However, EM and DLS analyses in the present study gave no indication for this. Even though the size distribution in all samples was somewhat heterogeneous, it is unlikely that the differences in effect of the polymers can

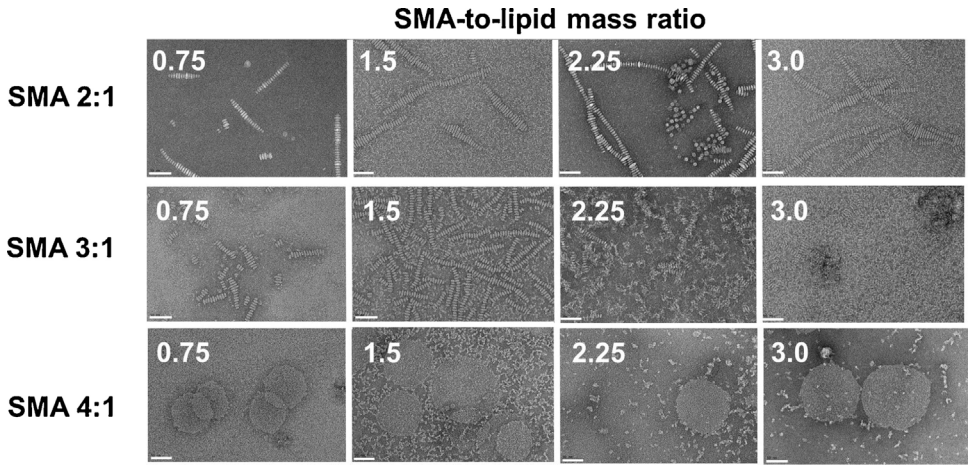

Fig. 6. Negative-stain transmission electron micrographs of di-16:0 PC nanodiscs bounded by SMA 2:1 (top), SMA 3:1 (middle) or SMA 4:1 (bottom). The scale bar corresponds to 50 nm. Nanodiscs were obtained at different SMA-to-lipid mass ratio as indicated in the figure.

be ascribed to a difference in size of the nanodiscs. We speculate that these effects are due to differences in polymer composition. SMA 3:1 and SMA 4:1 have a more inhomogeneous distribution of styrene and maleic acid units along their sequence as compared to SMA 2:1 (Scheidelaar et al., 2016). This would result in a more inhomogeneous membrane partitioning and thus might explain the larger broadening and lower T_m for SMA 3:1 and SMA 4:1 nanodiscs as compared to SMA 2:1 nanodiscs.

Further DSC analysis resulted in a remarkable observation that SMA 2:1 nanodiscs have the lowest calorimetric enthalpy, as was observed for all phosphatidylcholines tested when compared with SMA 3:1 and for di-16:0 PC lipids at different concentrations of SMA 2:1, SMA 3:1 or SMA 4:1. This effect would be consistent with a smaller size of the SMA 2:1 nanodiscs, in analogy to effects observed for MSP nanodiscs, where it was found that the calorimetric enthalpy in nanodiscs systematically increases with increasing size of the nanodiscs (Denisov et al., 2005). We speculate that also these effects are due to differences in polymer composition. Using nanodiscs bounded by SMA 3:1 it has been shown that insertion of styrenes into gel phase lipids is thermodynamically more favorable than insertion into fluid phase lipids, demonstrating that there are differences in polymer–lipid interactions as function of the phase state of the lipids in the nanodiscs (Cuevas Arenas et al., 2016). Indeed, insertion of the styrenes inbetween the lipid acyl chains can be expected to be less favorable for lipids in a fluid phase than for lipids in a gel phase, because in the fluid phase the chains will occupy more space causing steric hindrance. This effect will become stronger when the lipids are longer and when there is a higher density of styrenes. We therefore propose that the relatively large enthalpy for SMA 3:1 and SMA 4:1 nanodiscs is due a change in organization of the polymer around the rim of the nanodisc, which accompanies phase interconversion and which energetically contributes to the transition. This might also be the basis for the complex thermograms obtained for di-20:0 PC SMA 3:1-nanodiscs and for di-18:0 PC SMA 4:1-nanodiscs, where the main peak of the thermogram is split into two peaks. If there indeed is such a contribution, then this would imply that calculations of the cooperative unit as number of lipids participating in the phase transition (Oluwole et al., 2017; Orwick et al., 2012) are not useful in SMA-nanodiscs, because they are based on broadening and enthalpy values of a lipid melting transition only. It must be noted that this energetic contribution can not be interpreted as a gel-to-ripple phase pretransition since such ripples exclusively occur in pure extended lipid bilayer systems (i.e MLVs or supported lipid bilayers) and they are easily abolished by the presence of membrane-interacting molecules (Heimburg 2000). Furthermore, the pretransition can be considered as a macroscopic reorganization of lipids and since the periodicity of the ripples is at least ~5 times larger than the size of nanodiscs (Czajkowsky et al., 1995; Heimburg 2000) their presence in nanodiscs is highly improbable.

Another relevant finding in this manuscript is that the morphological integrity of the nanodiscs can be affected by increasing concentrations of SMA, depending on the hydrophobicity of the polymer. For SMA 2:1 nanodiscs no notable effect of varying the SMA concentration was observed, but for SMA 3:1 at higher SMA concentration regular discs could no longer be observed. Based on both EM and DLS analysis, SMA 4:1 nanodiscs do not appear to self-assemble in regular circular nanodiscs at any SMA concentration, but rather tend to form aggregates. Thus, the term nanodiscs may be incorrect for solubilized SMA 4:1 particles.

In conclusion, the data presented here suggest that the SMA 2:1 polymer is able to preserve native lipid packing properties in the nanodiscs to a higher extent than the SMA 3:1 polymer. Together with recent studies showing that SMA 2:1 is also more efficient in solubilizing membranes (Morrison et al., 2016; Scheidelaar et al., 2016), this supports the notion that SMA 2:1 is more suitable as tool for characterization of membrane proteins in native nanodiscs.

Acknowledgements

This work was supported financially by NWO Chemical Sciences, ECHO grants No. 711-013-005 (J.J.D.P) and 711-013-004 (M.F.R) and by the Seventh Framework Program of the European Union (Initial Training Network “ManiFold,” Grant 317371) (J.M.D). This work used the platforms of the Grenoble Instruct centre (ISBG;UMS 3518 CNRS-CEA-UJF-EMBL) with support from FRISBI (ANR-10-INSB-05-02) and GRAL (ANR-10-LABX-49-01) within the Grenoble partnership for structural biology (PSB). We thank Stefan Scheidelaar and Cornelis A. Van Walree (both from Utrecht University) for helpful discussions. We are very grateful to Dr. C. Moriscot and to Guy Schoehn, both from the Electron Microscopy platform of the Integrated Structural Biology of Grenoble (ISBG, UMI3265) for performing the TEM imaging.

References

Biltonen, R.L., Lichtenberg, D., 1993. The use of differential scanning calorimetry as a tool to characterize liposome preparations. Chemistry and physics of lipids 64 (1–3), 129–142. http://dx.doi.org/10.1016/0009-3084(93)90062-8.

Cuevas Arenas, R., Klingler, J., Vargas, C., Keller, S., 2016. Influence of lipid bilayer properties on nanodisc formation mediated by styrene/maleic acid copolymers. Nanoscale 32, 15016–15026. http://dx.doi.org/10.1039/c6nr02089e.

Czajkowsky, D.M., Huang, C., Shao, Z., 1995. Ripple phase in asymmetric unilamellar bilayers with saturated and unsaturated phospholipids. Biochemistry 34 (39), 12501–12505. http://dx.doi.org/10.1021/bi00039a003.

Denisov, I.G., McLean, M.A., Shaw, A.W., Grinkova, Y.V., Sligar, S.G., 2005. Thermotropic phase transition in soluble nanoscale lipid bilayers. The journal of physical chemistry. B 109 (32), 15580–15588. http://dx.doi.org/10.1021/jp051385g.

Dominguez Pardo, J.J., Dörr, J.M., Iyer, A., Cox, R.C., Scheidelaar, S., Koorengevel, M.C., Subramaniam, V., Killian, J.A., 2017. Solubilization of lipids and lipid phases by the

styrene-maleic acid copolymer. European biophysics journal: EBJ 1, 91–101. http://dx.doi.org/10.1007/s00249-016-1181-7.
Dörr, J.M., Koorengevel, M.C., Schafer, M., Prokofyev, A.V., Scheidelaar, S., van der Cruijsen, Elwin A W, Dafforn, T.R., Baldus, M., Killian, J.A., 2014. Detergent-free isolation, characterization, and functional reconstitution of a tetrameric K+ channel: the power of native nanodiscs. Proceedings of the National Academy of Sciences of the United States of America 111 (52), 18607–18612. http://dx.doi.org/10.1073/pnas.1416205112.
Dörr, J.M., Scheidelaar, S., Koorengevel, M.C., Dominguez, J.J., Schafer, M., van Walree, C.A., Killian, J.A., 2016. The styrene-maleic acid copolymer: a versatile tool in membrane research. European biophysics journal: EBJ 45 (1), 3–21. http://dx.doi.org/10.1007/s00249-015-1093-y.
Goto, M., Ishida, S., Tamai, N., Matsuki, H., Kaneshina, S., 2009. Chain asymmetry alters thermotropic and barotropic properties of phospholipid bilayer membranes. Chemistry and physics of lipids 161 (2), 65–76. http://dx.doi.org/10.1016/j.chemphyslip.2009.07.003.
Heimburg, T., 2000. A Model for the Lipid Pretransition: Coupling of Ripple Formation with the Chain-Melting Transition. Biophysical Journal 78 (3), 1154–1165. http://dx.doi.org/10.1016/S0006-3495(00)76673-2.
Jamshad, M., Grimard, V., Idini, I., Knowles, T.J., Dowle, M.R., Schofield, N., Sridhar, P., Lin, Y., Finka, R., Wheatley, M., Thomas, O.R.T., Palmer, R.E., Overduin, M., Govaerts, C., Ruysschaert, J.-M., Edler, K.J., Dafforn, T.R., 2015. Structural analysis of a nanoparticle containing a lipid bilayer used for detergent-free extraction of membrane proteins. Nano Res. 8 (3), 774–789. http://dx.doi.org/10.1007/s12274-014-0560-6.
Kemmer, G., Keller, S., 2010. Nonlinear least-squares data fitting in Excel spreadsheets. Nature protocols 5 (2), 267–281. http://dx.doi.org/10.1038/nprot.2009.182.
Lewis, Ruthven N.A.H., Mak, N., McElhaney, R.N., 1987. A differential scanning calorimetric study of the thermotropic phase behavior of model membranes composed of phosphatidylcholines containing linear saturated fatty acyl chains. Biochemistry 26 (19), 6118–6126. http://dx.doi.org/10.1021/bi00393a026.
Long, A.R., O'Brien, C.C., Malhotra, K., Schwall, C.T., Albert, A.D., Watts, A., Alder, N.N., 2013. A detergent-free strategy for the reconstitution of active enzyme complexes from native biological membranes into nanoscale discs. BMC biotechnology 13, 41. http://dx.doi.org/10.1186/1472-6750-13-41.
Marsh, D., 2013. Handbook of lipid bilayers, Second edition. CRC Press Boca Raton.
Morrison, K.A., Akram, A., Mathews, A., Khan, Z.A., Patel, J.H., Zhou, C., Hardy, D.J., Moore-Kelly, C., Patel, R., Odiba, V., Knowles, T., Javed, M.-U.-H., Chmel, N.P., Dafforn, T.R., Rothnie, A.J., 2016. Membrane protein extraction and purification using styrene-maleic acid (SMA) co-polymer: Effect of variations in polymer structure. Biochemical journal. http://dx.doi.org/10.1042/BCJ20160723.
Oluwole, A.O., Danielczak, B., Meister, A., Babalola, J.O., Vargas, C., Keller, S., 2017. Solubilization of Membrane Proteins into Functional Lipid-Bilayer Nanodiscs Using a Diisobutylene/Maleic Acid Copolymer. Angewandte Chemie (International ed. in English) 7, 1919–1924. http://dx.doi.org/10.1002/anie.201610778.
Orwick, M.C., Judge, P.J., Procek, J., Lindholm, L., Graziadei, A., Engel, A., Grobner, G., Watts, A., 2012. Detergent-free formation and physicochemical characterization of nanosized lipid-polymer complexes: Lipodisq. Angewandte Chemie (International ed. in English) 19, 4653–4657. http://dx.doi.org/10.1002/anie.201201355.
Parasassi, T., Di Stefano, M., Loiero, M., Ravagnan, G., Gratton, E., 1994. Influence of cholesterol on phospholipid bilayers phase domains as detected by Laurdan fluorescence. Biophysical Journal 66 (1), 120–132. http://dx.doi.org/10.1016/S0006-3495(94)80763-5.
Parasassi, T., Ravagnan, G., Rusch, R.M., Gratton, E., 1993. Modulation and dynamics of phase properties in phospholipid mixtures detected by laurdan fluorescence. Photochem Photobiol 57 (3), 403–410. http://dx.doi.org/10.1111/j.1751-1097.1993.tb02309.x.
Parasassi, T., Stasio de, G., Ravagnan, G., Rusch, R.M., Gratton, E., 1991. Quantitation of lipid phases in phospholipid vesicles by the generalized polarization of Laurdan fluorescence. Biophysical Journal. 1, 179–189. http://dx.doi.org/10.1016/S0006-3495(91)82041-0.
Prabudiansyah, I., Kusters, I., Caforio, A., Driessen, A.J.M., 2015. Characterization of the annular lipid shell of the Sec translocon. Biochimica et biophysica acta 1848 (10 Pt A), 2050–2056. http://dx.doi.org/10.1016/j.bbamem.2015.06.024.
Rouser, G., Fleischer, S., Yamamoto, A., 1970. Two dimensional thin layer chromatographic separation of polar lipids and determination of phospholipids by phosphorus analysis of spots. Lipids 5 (5), 494–496. http://dx.doi.org/10.1007/bf02531316.
Scheidelaar, S., Koorengevel, M.C., Dominguez, J.J., Meeldijk, J.D., Breukink, E., Killian, J.A., 2015. Molecular Model for the Solubilization of Membranes into Nanodisks by Styrene Maleic Acid Copolymers. Biophysical Journal 2, 279–290. http://dx.doi.org/10.1016/j.bpj.2014.11.3464.
Scheidelaar, S., Koorengevel, M.C., van Walree, C.A., Dominguez, J.J., Dörr, J.M., Killian, J.A., 2016. Effect of Polymer Composition and pH on Membrane Solubilization by Styrene-Maleic Acid Copolymers. Biophysical Journal 111 (9), 1974–1986. http://dx.doi.org/10.1016/j.bpj.2016.09.025.
Shaw, A.W., McLean, M.A., Sligar, S.G., 2004. Phospholipid phase transitions in homogeneous nanometer scale bilayer discs. FEBS letters 556 (1-3), 260–264. http://dx.doi.org/10.1016/S0014-5793(03)01400-5.
Swainsbury, D.J.K., Scheidelaar, S., van Grondelle, R., Killian, J.A., Jones, M.R., 2014. Bacterial reaction centers purified with styrene maleic acid copolymer retain native membrane functional properties and display enhanced stability. Angewandte Chemie (International ed. in English) 44, 11803–11807. http://dx.doi.org/10.1002/anie.201406412.
Tanaka, M., Hosotani, A., Tachibana, Y., Nakano, M., Iwasaki, K., Kawakami, T., Mukai, T., 2015. Preparation and Characterization of Reconstituted Lipid-Synthetic Polymer Discoidal Particles. Langmuir: the ACS journal of surfaces and colloids 31 (46), 12719–12726. http://dx.doi.org/10.1021/acs.langmuir.5b03438.
Zhang, L., Song, J., Cavigiolio, G., Ishida, B.Y., Zhang, S., Kane, J.P., Weisgraber, K.H., Oda, M.N., Rye, K.-A., Pownall, H.J., Ren, G., 2011. Morphology and structure of lipoproteins revealed by an optimized negative-staining protocol of electron microscopy. Journal of lipid research 52 (1), 175–184. http://dx.doi.org/10.1194/jlr.D010959.